Crystallization of Syndiotactic Polystyrene in β-Form. 2. Quantification of Stacking Faults in the Solution-Grown Single Crystals

Noritaka Hamada,† Masatoshi Tosaka,* Masaki Tsuji, Shinzo Kohjiya, and Ken-ichi Katayama‡

Institute for Chemical Research, Kyoto University, Uji, Kyoto-fu 611, Japan

Received April 23, 1997; Revised Manuscript Received August 13, 1997⊗

ABSTRACT: The probability of the presence of stacking faults in the β-form single crystals of syndiotactic polystyrene, which were grown isothermally from a dilute solution at a temperature ranging from 150 to 210 °C, was estimated from the mean half-breadth of the streaked reflections. The probability was also estimated by counting the number of the faults recorded in the dark-field and the high-resolution electron microscopic images. The probability showed weak dependence on crystallization temperature, with its maximum value at 165 °C. When the single crystals grown at 165 °C were annealed isothermally even at 260 °C, only a small decrease in the amount of stacking faults was detected. The molecular mechanism of and difficulty in eliminating the stacking faults by annealing were discussed on the basis of the structural model of the fault.

Introduction

In four polymorphic forms[1−11] of syndiotactic polystyrene (s-PS), the β-form, according to the nomenclature by Guerra *et al.*,[5] is distinguished by an orthorhombic unit cell and a planar zigzag conformation of backbone chain. The crystal structure was analyzed and a disordered structure in the crystal was reported by Chatani *et al.*[12] and by De Rosa *et al.*[13] Independently, we had reported about the stacking fault in the β-form single crystal of s-PS grown isothermally from a dilute solution.[14,15] The existence of the stacking fault was readily deduced from certain characteristic features in the selected-area electron diffraction (ED) pattern. In the ED pattern of the β-form single crystal, $hk0$ reflections with $h + k =$ even are spotlike, while the others with $h + k =$ odd are streaked along the a^*-direction. Our structural model of the stacking fault[15] to explain the features in the ED pattern is schematically shown in Figure 1, in which a rectangle drawn with broken lines indicates the unit cell. In the model, the regular structure of the β-form is composed of two kinds of motifs. Each motif is then composed of two molecular layers extending parallel to the *bc*-plane, in particular in the *b*-axis direction, and its thickness in the *c*-axis direction approximately equals the lamellar thickness of the single crystal. The motifs are distinguished from each other by the rotational orientation of the planar-zigzag backbone chain around the chain axis. These two types of motifs are named A and B for convenience as shown in Figure 1, in which subscripts (1 and 2) show the relative shift along the *b*-axis by $b/2$. Here the regular crystal structure is defined as an alternating stack of these two motifs, and thus both sequences, $-A_1B_2A_1B_2-$ and $-A_2B_1A_2B_1-$ correspond to the regular structure. When a successive sequence of the same two motifs, such as $-B_1A_2A_1B_2-$ or $-A_1B_2B_1A_2-$ is incorporated into a stack, this sequence is defined as the stacking fault. For example, the sequence of

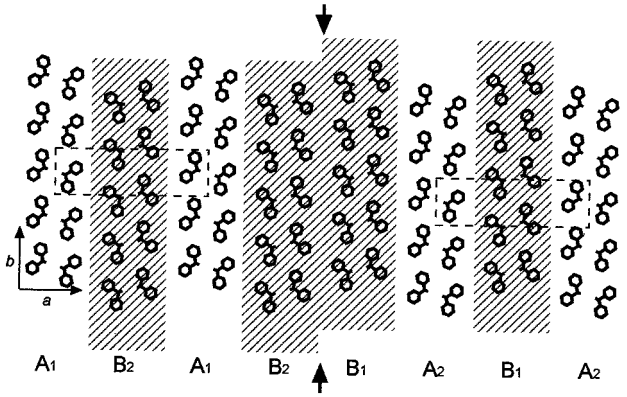

Figure 1. The *ab*-projection of the crystal structure of β-form s-PS with the stacking fault. The unit cell of the regular structure is shown by a rectangle drawn with broken lines. Motifs B are shaded. A pair of arrows indicate the position of the stacking fault.

$-B_1A_2A_1A_2A_1B_2-$ or $-A_1B_2B_1B_2B_1A_2-$ involves "three" stacking faults. Theoretical formulation of the intensity distribution based on this model explained sufficiently the characteristic features observed in the ED pattern.[15]

A similar model of the stacking fault was proposed by De Rosa *et al.*,[13] as well as by Chatani *et al.*[12] Chatani *et al.* roughly estimated the probability of presence of the stacking faults at 30% to explain the extinction rule of the crystal. As is deduced from our theoretical formulation, if the probability exceeds 50%, the reflections with $h + k =$ odd will disappear, and each of the reflections with $h + k =$ even ($k \neq 0$) will be overlapped with a streak.[14] This case is to correspond to the β' modification (disordered) reported by De Rosa *et al.*[5,13] This type of stacking fault is a rare case in polymer crystals, though there are many examples of stacking faults accompanying partial dislocations. It is, however, significant to study the behavior of the fault, *e.g.*, the change in their amount depending on the thermal history, from an academic point of view. It is also important to know, from the industrial viewpoint, the detailed structure of the β-form crystal, since this modification is observed in a melt-crystallized sample[5,11] and is expected to exist in injection-molded pieces.

In previous work,[15] we formulated the relation between the intensity profile in the ED pattern and the

* To whom all correspondence should be addressed: tel, +81-774-38-3063, fax, +81-774-38-3069; e-mail, tosaka@scl.kyoto-u.ac.jp.

† Present address: Yamanouchi Pharmaceutical Co., Ltd.

‡ Present address: Heian Jogakuin College.

⊗ Abstract published in *Advance ACS Abstracts,* October 1, 1997.

S0024-9297(97)00557-3 CCC: $14.00

probability of presence of the stacking faults. By extending the formulation in the reverse way, we may be able to calculate the probability from the real intensity profile of the streaked reflections in the ED pattern. On the other hand, we can also estimate the probability by counting directly the number of the faults recorded in the images obtained by high-resolution electron microscopy (HREM) and/or by a dark-field (DF) imaging technique.[16] In the present work, the stacking faults in s-PS single crystals are quantified by using these three techniques. Then the dependence of the probability in question on the crystallization and the annealing temperatures is discussed.

Theoretical Basis

The mathematical prediction of the diffraction intensity from the s-PS single crystal is cited below.[15] The fractional coordinates U, V, and W are defined to indicate a position in the reciprocal space, instead of the indices h, k and l. Here, V and W have only integer values because the planes of stacking fault in question are parallel to the crystallographic bc-plane in a sufficiently large crystal, but U may have any real value. Then f_{A_1}, f_{A_2}, f_{B_1}, and f_{B_2} are defined as the structure factors for the motifs A_1, A_2, B_1, and B_2 in Figure 1, respectively. If we define $f_{A_1} = f(U,V,W)$, the others are $f_{A_2} = f(U,V,W)\exp(i\pi V)$, $f_{B_1} = f(U,-V,W)$, and $f_{B_2} = f(U,-V,W)\exp(i\pi V)$. The probability of the presence of the stacking faults, namely, the probability that two of the same type of motifs are adjacently located, is written as p. Here the diffraction intensity $I(U,V,W)$ from a very large crystal is expressed as follows:

(a) V = even

$$I \propto \frac{J_1 + J_2}{2}\sum_n \delta(U - 2n) + \frac{J_1 - J_2}{2}\frac{1 - \epsilon^2}{1 - 2\epsilon\cos\{\pi(U+1)\} + \epsilon^2} \quad (1)$$

(b) V = odd

$$I \propto \frac{J_1 + J_2}{2}\sum_n \delta(U - 2n - 1) + \frac{J_1 - J_2}{2}\frac{1 - \epsilon^2}{1 - 2\epsilon\cos(\pi U) + \epsilon^2} \quad (2)$$

where $\epsilon = 1 - 2p$, $J_1 = (|f_{A_1}|^2 + |f_{B_1}|^2)/2$, $J_2 = (f_{A_1}{}^* f_{B_1} + f_{A_1} f_{B_1}{}^*)/2$, and δ is Dirac's delta-function. The asterisk (*) means the complex conjugate.

These equations for $I(U,V,W)$ sufficiently express the features in the ED pattern of the s-PS single crystal when $p < 0.5$. The summation terms in these equations correspond to the spotlike reflections with $h + k$ = even, and the last term in each equation represents the streaked reflections with $h + k$ = odd. When $p = 0.5$, both of the last terms in eqs 1 and 2 equal $(J_1 - J_2)/2$ and the streaks in the ED pattern will continuously spread over the whole range of U.[14] If $p > 0.5$, reflections with $h + k$ = odd will disappear and each of the spotlike reflections with $h + k$ = even will be overlapped with a streak. This change of the feature in the ED pattern is schematically shown in Figure 2.

As mentioned above, the last terms in eqs 1 and 2 represent the intensity profiles of the streaked reflections. Here we assume J_1 and J_2 to be constant in the range of U, which is assigned to one reciprocal lattice point. Then, ϵ is calculated from the half-breadth H (Figure 3) of the profile of each streaked reflection with the following equation:

$$\epsilon = 2 - \cos\pi H - \sqrt{(2 - \cos\pi H)^2 - 1} \quad (3)$$

Accordingly, quantification of the stacking faults can be achieved simply by measuring the half-breadth of streaked $hk0$ reflections. An as-measured value of the half-breadth includes the effect resulting from some additional factors other than the stacking faults (for example, instrumental broadening, broadening due to photodensitometry, etc.). We here further assume, therefore, that all the intensity profiles are Gaussian and that the degree of broadening due to the additional factors is represented by the half-breadth of the spotlike $hk0$ ($h + k$ = even) reflections. Then the effect due to

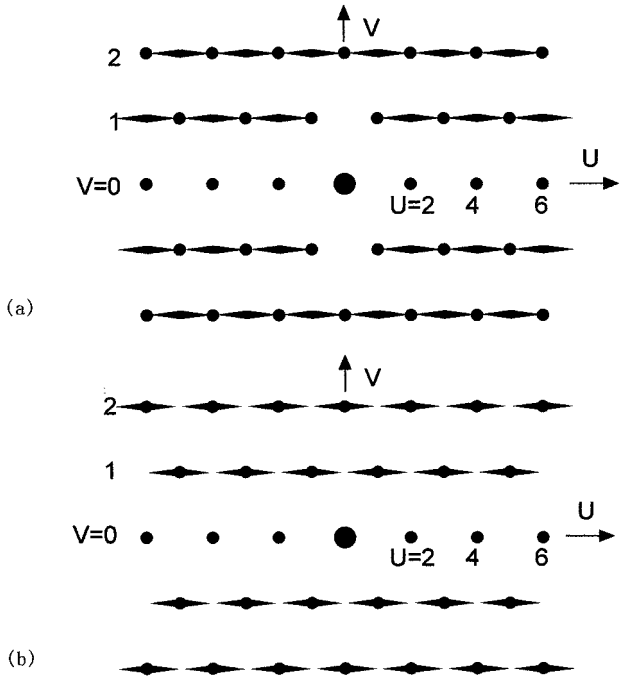

Figure 2. Schematic representation of the ED patterns depending on the value of p. (a) When $p < 0.5$, reflections with $h + k$ = even are spotlike, while the others with $h + k$ = odd are streaked along the a^*-direction. (b) When $p > 0.5$, reflections with $h + k$ = odd disappear and each of the spotlike reflections with $h + k$ = even is overlapped with a streak.

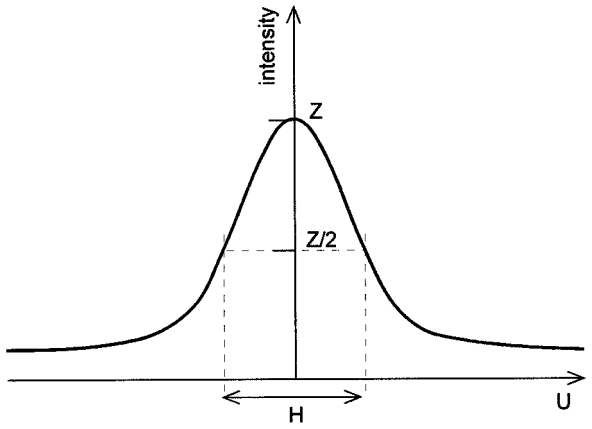

Figure 3. Intensity profile of a streaked reflection and the definition of its half-breadth H. For the reflection with the peak height Z, its half-breadth H is defined as the breadth at $Z/2$.

additional factors can be subtracted away from the as-measured half-breadth of streaked *hk0* reflections, and the residual corresponds to the half-breadth due to the stacking faults: hereafter H denotes this corrected mean value of the half-breadth due to the stacking faults which is averaged for several streaked reflections in one ED negative. In this way, we can quantify the stacking faults in the s-PS single crystal by converting the final value of the corrected mean half-breadth, H, into ϵ using eq 3, namely, into p ($=(1 - \epsilon)/2$).

Experimental Section

The s-PS ($M_w = 7 \times 10^4$) sample was kindly supplied by Idemitsu Petrochemical Co., Ltd., and was used without further purification. Single crystals of s-PS were prepared on the NaCl (001) face from an 0.01 wt % solution of the mixed solvent (*n*-tetradecane/decahydronaphthalene, 2:1 v/v) according to the procedure in ref 16, by isothermal crystallization at a temperature ranging from 150 to 225 °C. Some single crystals grown at 165 °C were placed on a hot plate before removal of NaCl, and then annealed in air at a given temperature ranging from 170 to 260 °C. Then the NaCl with s-PS crystals which were reinforced with vapor-deposited carbon was put into water, and the s-PS specimen was floated away from NaCl and picked up onto a copper grid for transmission electron microscopy (TEM).

The specimens thus prepared were investigated with a transmission electron microscope (JEOL JEM-200CS) operated at 200 kV, and ED patterns and bright-field and DF images were obtained at room temperature. The distribution of diffraction intensity in the ED pattern was measured by the following three methods.

(A) Each ED pattern from a circular region (about 9.4 μm in diameter) of the s-PS single crystal was recorded on electron microscopic film (Mitsubishi MEM). Then the optical density distribution of the pattern in the film was measured with a microdensitometer (Joyce-Loebl MK III CS) and plotted on a sheet of graph paper. Optical density thus measured was regarded directly as diffraction intensity, and the half-breadth of each diffraction maximum was read out from the plot.

(B) Each ED pattern from a smaller circular region (about 3 μm in diameter) of the crystal was recorded on a MEM film. Then the optical density distribution in the ED pattern was measured with a microdensitometer (Perkin-Elmer PDS 1010), and digital data were transferred into a computer. As in (A), optical density was regarded directly as diffraction intensity. Then the intensity profile of each diffraction maximum was fitted by a Gaussian curve, and its corresponding half-breadth was obtained.

(C) Each ED pattern was recorded as a set of graphic data into a personal computer through a TV system (GATAN 622SC) connected to the JEM-200CS. The same size of the selected-area aperture as in (B) was utilized (about 3 μm in diameter in the object plane). Then the intensity distribution was directly read out from the graphic data. The half-breadth of each diffraction maximum was obtained by processing these data as in (B).

For electron microscopic films, the relationship between the optical density, D, and the electron exposure, Q, has already been investigated, and D is directly proportional to Q up to $D = ca.\ 1.5$.[17] In our experiments here, accordingly, their linear range ($0 \le D < 1.5$) was utilized.

DF images and high-resolution images were taken according to the procedures detailed in our previous reports.[15,16]

Results and Discussion

Single crystals with fairly large monolayered areas were obtained at crystallization temperatures below 210 °C. ED patterns mainly from these monolayered areas were used for further investigation. Figure 4 shows an example of the intensity distribution along the a^*-direction in the ED pattern of s-PS single crystal. In this figure, maxima which are pointed by arrowheads correspond to streaked reflections. The mean half-breadth of streaked reflections with $h + k =$ odd and that of spotlike reflections with $h + k =$ even were calculated for every ED pattern. Then the corrected mean half-breadth, H, was computed from these mean half-breadths.

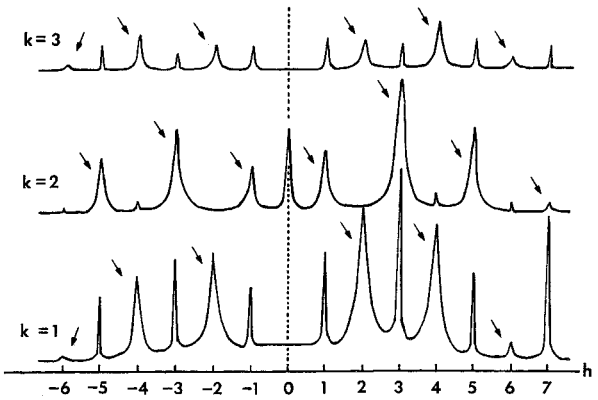

Figure 4. An example of as-measured intensity distribution of the reflections along the a^*-axis, namely, their optical density distribution in a typical ED negative. Streaked reflections are pointed by arrowheads.

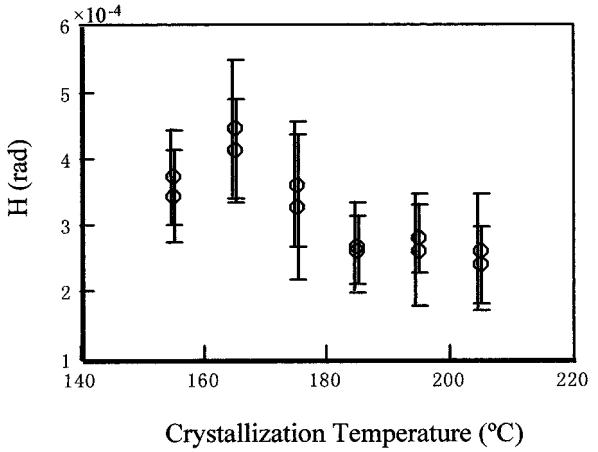

Figure 5. Dependence of corrected half-breadth H on crystallization temperature. Each circle corresponds to the mean value averaged for several streaked reflections in one ED negative. Vertical bars represent standard deviations.

Isothermal Crystallization. Figure 5 shows the dependence of H on crystallization temperature; here, H was estimated by method A. The corrected mean half-breadth H decreased, to some extent, as increasing crystallization temperature. From this figure, we deduce that the amount of stacking faults decreased with an increase in the temperature. Then the data were converted to the temperature dependence of the probability of the presence of the faults, p, according to eq 3. The result was plotted in Figure 6 using the open circles, and will be discussed later together with the probabilities estimated by the other methods.

We could obtain the HREM images from which the location of the faults was detected. At the fault, (210) lattice fringes are shifted by half a period along the *b*-direction.[15,16] In addition, we found irregularly spaced parallel striations running in the *b*-direction in the DF images: According to the computer simulation, each striation corresponds to the position of the stacking fault.[16] The probability of presence of the stacking faults, p, was directly estimated from HREM and DF images by counting the number of the faults in a unit length along the *a*-axis of the crystal.

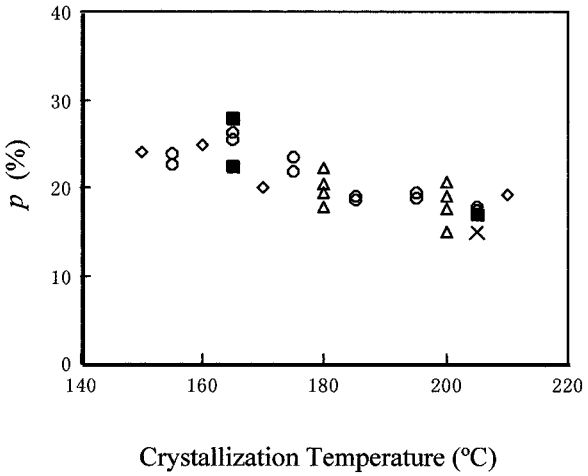

Figure 6. Dependence of p on crystallization temperature. The methods to estimate p values are as follows: ○, ED (A); ◇, ED (B); △, ED (C); ×, HREM; ■, DF.

The number of the faults that is read out from these DF and HREM images is comparatively indisputable, except that we might have more or less underestimated the number of the faults in the DF images because of the difficulty to identify separately two or more faults which are close to each other, in particular to identify respective neighboring faults in a consecutive sequence of them. However both of the HREM and DF methods are rather difficult to perform and less reproducible because of the radiation damage. On the other hand, we can surely derive the probability value by ED, but the reliability of the value must be examined by other methods since we have introduced some approximations to derive the probability, p. Hence we adopted the HREM and DF methods only to obtain values of p for the crystals isothermally grown at a few selected crystallization temperatures, and resultant p values were regarded as references to evaluate the reliability of the values obtained by ED. Even though there were some approximations in the process to estimate the probability by ED, the value thus estimated agreed well with those obtained from DF and HREM images.

Figure 6 shows the values of p obtained by different methods which are plotted as a function of crystallization temperature. The deviation of p at a given crystallization temperature was within ±3% from the mean value. The values of p estimated from the greater specimen area (*viz.*, by method A) showed smaller deviation. Hence it is concluded that the deviation of p is to result from local fluctuation in the frequency of presence of the stacking faults. In this experiment, p showed weak dependence on the crystallization temperature, with a maximum value of 26% at 165 °C. Even if the plot is extended to the higher temperatures beyond 210 °C, p will not fall to 0% below the boiling temperature of the solvent. The boiling temperature of the solvent is around 230 °C, and s-PS must be dissolved below the temperature. If we assume that defect-free single crystals can grow below the boiling temperature of the solvent, an abrupt drop of p must occur between 210 and 230 °C. The propriety of this expectation will be discussed on the basis of energetic difference between regular and faulted structures[8,10] in our future publication.

Annealing Experiment. Since the s-PS single crystals grown at 165 °C showed the maximum value of p, as shown in Figure 6, they were annealed, and the change in the amount of the stacking faults was examined. Figure 7 shows the dependence of H on

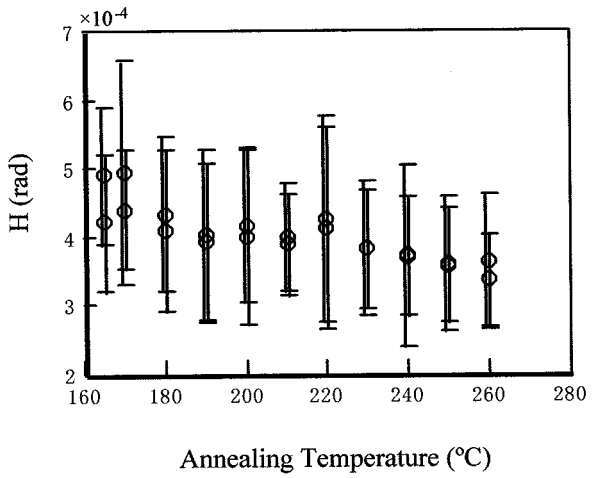

Figure 7. Dependence of corrected half-breadth H on annealing temperature. Each circle corresponds to the mean value averaged for several streaked reflections in one ED negative. Vertical bars represent standard deviations. The specimens were isothermally grown at 165 °C and annealed for 2 h in air.

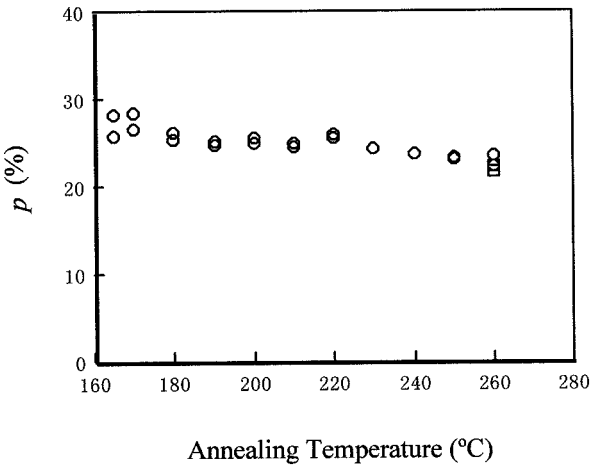

Figure 8. Dependence of p on annealing temperature. The specimens were isothermally grown at 165 °C and annealed for 2 h in air (circle) or 48 h *in vacuo* (square). The p values were estimated from the ED patterns by method A.

annealing temperature which was obtained by ED by method A. Only a slight decrease in broadening of the streaked reflections along the a^*-direction was observed.

Figure 8 shows the values of p plotted as a function of annealing temperature, which were converted from Figure 7 with eq 3. The p values decreased with increasing annealing temperature. However the dependence of p on annealing temperature is weaker than that on crystallization temperature (compare Figure 8 with Figure 6). Annealing seems to have eliminated only a small amount of stacking faults, even when the crystals were annealed at a temperature up to 260 °C. (The melting temperature of the crystals is around 270 °C, but they start to melt at around 260 °C. The melting behavior of this crystal is complicated.[18−20]) Additional annealing experiment at 260 °C for 48 h *in vacuo* showed essentially no further decrease in the p value, and the result is plotted in Figure 8 by the open square. The stacking faults are eliminated, therefore, at a rate which is not constant but falls down rapidly (almost to be zero) after a certain amount of the faults are eliminated.

The annealing behavior of the β-form single crystals of s-PS is explained qualitatively on the basis of our

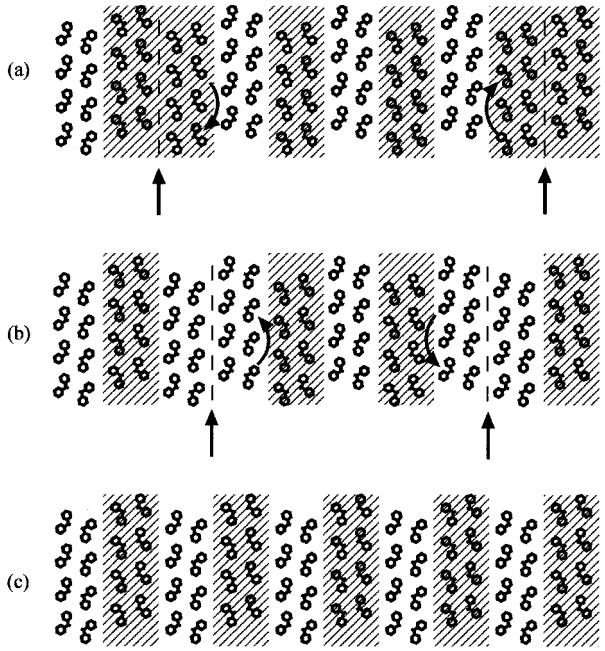

Figure 9. Schematic illustration which demonstrates the elimination of stacking faults. Motifs B are shaded as in Figure 1. Rotation of the stems around their axis, which are normal to the plane of this figure, to cancel one fault (a) results in another fault (b). Collision between two faults can eliminate them and yield the regular structure (c).

model of the fault, as illustrated in Figure 9. If the molecular motion, which is enhanced thermally, results in rotation of all the stems around their own molecular axis in a motif next to the stacking fault, then the fault at the original position is expected to be eliminated. However, this molecular motion makes another stacking fault next to the original position (Figure 9a); *i.e.*, a stacking fault can only move to the right or left from its original position but cannot be eliminated by this motion in one motif. The probability that a stacking fault moves to the right from its original position is, of course, identical with that to the left, and this movement does not change the total energy of the single crystal unless the fault is eliminated from the crystal. Consequently, the fault might stay at or near its original position. When a fault has come to the edge of the crystal, strictly speaking, to the edge of the crystallite, it will be excluded from and therefore can be eliminated from the crystallite. When two faults collide with each other (parts b and c of Figure 9), they can be eliminated together. The rotation of the stems seems to be difficult, because there is no energetic gain in the system; *i.e.*, there is no thermodynamic driving force unless the fault is eliminated, as mentioned above. When two stacking faults are located at the adjacent positions, the system can have a free energy gain by eliminating them. This case may correspond to the decrease of p in the annealing experiment. When, for example, three consecutive stacking faults are at the adjacent positions, two of them can eliminate themselves but one of them is left without any "partner". The following equation gives the probability Δp that the consecutive $2n$ stacking faults (n: integer) are in the crystal that is to have the probability of presence of stacking faults, p

$$\Delta p \equiv \sum_{n=1}^{\infty} p^{2n}(1-p) = p^2/(1+p) \qquad (4)$$

Since these consecutive $2n$ stacking faults can be eliminated by annealing, the expected probability decrease is also given by Δp. Indeed, using this equation, Δp is computed at 5.2% for the initial (*viz.* unannealed) specimen grown at 165 °C, which agrees well with an about 5% drop in p between for the initial specimen and for the specimen annealed at 260 °C for 48 h. This quantitative coincidence suggests strongly that isolated stacking faults in the as-grown single crystals were not eliminated by annealing. Once the stacking faults are incorporated in the crystal, therefore, it might be very difficult to eliminate them perfectly only by annealing.

Conclusion

The probability, p, of the presence of the stacking faults in the β-form single crystal of s-PS was estimated. The values of p derived by three different methods presented here are in good agreement with each other. The dependence of p on the crystallization temperature was so weak that the p value seems not to fall to 0% even near the dissolving temperature of the crystal into the solvent. Even if the dried sample was isothermally annealed at a given temperature up to 260 °C, the elimination of the faults hardly occurred. These results suggest that it is difficult to obtain the fault-free crystal of the β-form.

Acknowledgment. The authors are grateful to Idemitsu Petrochemical Co., Ltd., for providing the s-PS sample used in this study and to Professor H. Kurokawa of Kwasan Observatory of Kyoto University and Professor R. Saitoh of Ryukoku University for obtaining the data of optical density distribution with PDS 1010 in KIPS (Kwasan Image Processing System).

References and Notes

(1) Chatani, Y.; Fujii, Y.; Shimane, Y.; Ijitsu, T. *Polym. Prepr., Jpn.* **1988**, *37*, 1179.
(2) Shimane, Y.; Ishioka, T.; Chatani, Y.; Ijitsu, T. *Polym. Prepr., Jpn.* **1988**, *37*, 2534.
(3) Grassi, A.; Longo, P.; Guerra, G. *Makromol. Chem., Rapid Commun.* **1989**, *10*, 687.
(4) Guerra, G.; Musto, P.; Karasz, F. E.; MacKnight, W. J. *Makromol. Chem.* **1990**, *191*, 2111.
(5) Guerra, G.; Vitagliano, V. M.; De Rosa, C.; Petraccone, V.; Corradini, P. *Macromolecules* **1990**, *23*, 1539.
(6) Gomez, M. A.; Tonelli, A. E. *Macromolecules* **1991**, *24*, 3533.
(7) Wang, Y. K.; Savage, J. D.; Yang, D.; Hsu, S. L. *Macromolecules* **1992**, *25*, 3659.
(8) Capitani, D.; De Rosa, C.; Ferrando, A.; Grassi, A.; Segre, A. L. *Macromolecules* **1992**, *25*, 3874.
(9) Chatani, Y.; Shimane, Y.; Inoue, Y.; Inagaki, T.; Ishioka, T.; Ijitsu, T.; Yukinari, T. *Polymer* **1992**, *33*, 488.
(10) Deberdt, F.; Berghmans, H. *Polymer* **1993**, *34*, 2192.
(11) Kellar, E. J. C.; Galiotis, C.; Andrews, E. H. *Macromolecules* **1996**, *29*, 3515.
(12) Chatani, Y.; Shimane, Y.; Ijitsu, T.; Yukinari, T. *Polymer* **1993**, *34*, 1625.
(13) De Rosa, C.; Rapacciuolo, M.; Guerra, G.; Petraccone, V.; Corradini, P. *Polymer* **1992**, *33*, 1423.
(14) Tosaka, M.; Tsuji, M.; Kawaguchi, A.; Katayama, K.; Iwatsuki, M. *Polym. Prepr., Jpn.* **1988**, *37*, 2564.
(15) Tsuji, M.; Okihara, T.; Tosaka, M.; Kawaguchi, A.; Katayama, K. *MSA Bull.* **1993**, *23*, 57.
(16) Tosaka, M.; Hamada, N.; Tsuji, M.; Kohjiya, S.; Ogawa, T.: Isoda, S.; Kobayashi, T. *Macromolecules* **1997**, *30*, 4132.
(17) Tsuji, M.; Kohjiya, S. *Prog. Polym. Sci.* **1995**, *20*, 259.
(18) Arnauts, J.; Berghmans, H. *Polym. Commun.* **1990**, *31*, 343.
(19) Gvozdic, N. V.; Meier, D. J. *Polym. Commun.* **1991**, *32*, 183.
(20) Gvozdic, N. V .; Meier, D. J. *Polym. Commun.* **1991**, *32*, 493.
(21) Cimmino, S.; Di Pace, E.; Martuscelli, E.; Silvestre, C. *Polymer* **1991**, *32*, 1080.

MA9705578